International Journal of Thermodynamics (IJoT)
ISSN 1301-9724 / e-ISSN 2146-1511
https://dergipark.org.tr/en/pub/ijot

Vol. 28 (No. 3), pp. 196-204, 2025
doi: 10.5541/ijot.1624762
Published online: September 1, 2025

Research Article

R1233zd(E) and Dimethylacetamide-based Diffusion Absorption Cooling System

[1*]B. Gurevich, [1]A. Zohar

[1]Shamoon College of Engineering, 84 Jabotinsky St., Ashdod 77245, Israel
E-mail: *bellagu@sce.ac.il

Received 22 January 2025, Revised 24 June 2025, Accepted 14 July 2025

Abstract

This study investigates the feasibility of utilizing 1-Chloro-3,3,3-trifluoropropene (R1233zd(E)) as the refrigerant and Dimethylacetamide (DMAC) as the absorbent in a Diffusion Absorption Refrigeration (DAR) system. The thermodynamic properties of the R1233zd(E)-DMAC binary solution were experimentally determined, including pressure-temperature-concentration and enthalpy-temperature-concentration data. These experimentally obtained data were integrated into a detailed DAR system model. Simulations were conducted to evaluate system performance, focusing on the influence of generator temperature and solution concentrations on the Coefficient of Performance (COP) and circulation ratio. In addition, an exergy analysis was conducted. This approach allowed for identifying the locations and magnitudes of exergy losses and evaluating overall efficiency based on useful energy quality. The results demonstrate that the system exhibits a COP value of 0.4 at an optimal generator temperature of 114°C. This optimal temperature is significantly lower than that typically observed in conventional ammonia-water systems or other HFC-based DAR systems. Moreover, the system operates at considerably lower pressures. This study contributes valuable insights into the potential of R1233zd(E)-DMAC as a promising working fluid pair for sustainable and energy-efficient DAR systems, particularly those utilizing low-grade heat sources.

Keywords: *Vapor liquid equilibrium; binary solutions; 1-chloro-3,3,3-trifluoropropene (R1233zd(E)) and Dimethylacetamide (DMAC); thermodynamic properties; diffusion absorption cooling systems.*

1. Introduction

The first diffusion absorption refrigerator (DAR) was developed in 1928 and employed a combination of ammonia as the refrigerant, water as the absorbent, and hydrogen as an auxiliary inert gas [1]. Since then, ammonia–water binary mixtures have remained the most widely used working pair in DAR systems due to their high latent heat of evaporation and low freezing point, which enable effective operation at low evaporator temperatures. The thermodynamic properties of this mixture have been extensively studied, forming the basis for system design, optimization, and simulation. This includes the development of generalized equations of state [2], experimental determination of enthalpy, entropy, and specific volume data [3], and the creation of computational tools such as AMMWAT, based on Gibbs free energy formulations [4]. Improved vapor–liquid equilibrium (VLE) modeling was achieved using modified Peng–Robinson equations [5], validated by wide-range experimental data [6]. Additional work has addressed energy balances and equilibrium states [7] and proposed dedicated equations of state to improve thermodynamic modeling accuracy across a range of conditions [8]. Building upon these foundations, extensive research has focused on improving DAR systems' performance using simulation and experimentation. Studies have confirmed the feasibility of using DAR systems with low-grade heat sources such as solar or waste heat [9]. Enhanced thermodynamic models have been developed to optimize heat exchanger integration and increase the coefficient of performance (COP) [10]. Experimental investigations reported typical rich solution concentrations in the range of 0.3–0.4 and COP values between 0.1 and 0.4, depending on system design and thermal insulation [11,12]. The 'rich' solution refers to the absorbent-refrigerant mixture exiting the absorber with a higher refrigerant mass fraction, while the 'poor' solution corresponds to the mixture exiting the generator after partial desorption, containing a lower refrigerant content.

To overcome the limitations of ammonia–water systems—namely, high operating pressures, toxicity, and corrosiveness—researchers have investigated alternative working fluid pairs composed of hydrofluorocarbons (HFCs) or hydrofluoroolefins (HFOs) combined with organic solvents. Numerical investigations of DAR systems using the R124–DMAC working pair demonstrated promising thermal behavior, with activation temperatures ranging from 80 °C to 180 °C and significantly lower vapor pressures than DMF-based mixtures [13, 14]. Parametric studies showed that optimal performance occurred at generator temperatures between 120 °C and 150 °C, with reduced COP observed at higher temperatures due to increased heat input, and improved performance achieved when poor solution concentrations were minimized [15]. Comparative evaluations of organic refrigerants such as R134a and R124, paired with DMAC, confirmed that while these systems operate at lower pressures and with improved safety, they generally require higher generator temperatures (around 150 °C) and exhibit slightly lower COPs than ammonia–water systems [16]. These refrigerant–absorbent pairs also

*Corresponding Author

offer reduced toxicity, chemical stability, full miscibility, and the ability to operate at sub-zero evaporator temperatures—all of which make them attractive alternatives to ammonia–water mixtures [17]. Further work explored the performance of simplified DAR configurations using R22, R32, R124, R125, and R134a with DMAC and helium as the inert gas [16]. These systems showed similar COP trends and solution concentration behavior, although their generator temperatures were typically higher, and their efficiency was generally lower than conventional ammonia-based systems. Earlier efforts also examined binary mixtures of R134a with various organic absorbents—including DMETEG, MCL, and DMEU—to evaluate vapor–liquid equilibrium and excess enthalpy behavior [18]. Similarly, R124 was tested with DMAC, MCL, DMEU, DMETEG, and NMP, with thermophysical property analysis and enthalpy–concentration diagram development identifying R124–DMAC as the highest-performing pair in terms of COP and circulation ratio [19]. In parallel, growing environmental regulations such as the European F-Gas Regulation have prompted a transition from high-GWP refrigerants like R134a, R404A, and R410A toward more sustainable options [20]. As a result, low-GWP hydrofluoroolefins (HFOs) have gained increasing attention for use in vapor compression and absorption cycles. R1234yf has been extensively characterized for its vapor pressure, saturated densities, and specific heat capacities [21]. At the same time, R1234ze(Z) has been described using a fundamental equation of state, providing reliable modeling across a wide range of conditions [22]. Thermophysical data for R1336mzz(E), including saturation and enthalpy–entropy characteristics, have supported its application in low-temperature, high-efficiency systems [23]. For R1233zd(E), a comprehensive international standard equation of state was developed, covering temperatures from the triple point to 450 K and pressures up to 100 MPa, confirming its potential for low-grade heat utilization [24]. These advances have facilitated the implementation of HFO refrigerants in thermodynamic modeling tools such as EES, enabling system-level performance predictions for novel cycles. R1233zd(E), in particular, has already been tested as a working fluid in organic Rankine cycles [25], and its thermodynamic properties have been incorporated into EES using newly developed equations of state [26]. However, the literature on using HFOs in binary solutions with organic absorbents for diffusion absorption refrigeration remains sparse.

R1233zd(E) offers a significant environmental advantage over traditional HFC refrigerants, with a GWP of approximately one compared to values exceeding 1400 for R134a and 2000 for R410A. It also presents a safer alternative to ammonia (GWP = 0) due to its low toxicity and non-flammability [25].

One recent study experimentally investigated the R1234yf–DMAC system, providing temperature–pressure–concentration and enthalpy–temperature–concentration data [27], although the results have not yet been applied within a DAR model. Given these gaps, the present study aims to experimentally evaluate the R1233zd(E)–DMAC binary mixture by obtaining pressure–temperature–concentration and enthalpy–temperature–concentration data. These results will be implemented into a DAR system model to assess the feasibility and performance of this low-GWP working pair for use with low-grade thermal energy sources.

2. Experimental Data of Thermodynamic Properties

Thermodynamic properties depend on the refrigerant solution's concentration in a binary solution. Direct measurement of refrigerant concentrations within both the liquid and vapor phases presents a significant challenge. To address this, our procedure integrates experimental data with analytical tools, leveraging the fundamental principle of fugacity equality between the two phases as described in Eq. (1). Our previous work presents a more detailed procedure [27].

$$y_i p = \gamma_i x_i p_i^{sat} \Phi_i \tag{1}$$

The experimental setup consisted of a 300 mL Parr 4383 pressure vessel equipped with a controlled heating jacket and stirring, as shown in Figure 1. Measured masses of refrigerant R1233zd(E) and organic solvent DMAC were introduced into the vessel, and the target temperature was set. Equilibrium was reached when the temperature difference between the refrigerant and the solvent stabilized within 0.5°C. At equilibrium, the system pressure was recorded. Subsequently, the vessel was cooled, and the procedure was repeated at higher temperatures to cover the desired range. Once the experiments were completed for a specific refrigerant mass, a larger quantity of refrigerant was added to the system, and the entire series of experiments was repeated to encompass the desired range of refrigerant masses. Note that the mass of the solvent remained constant.

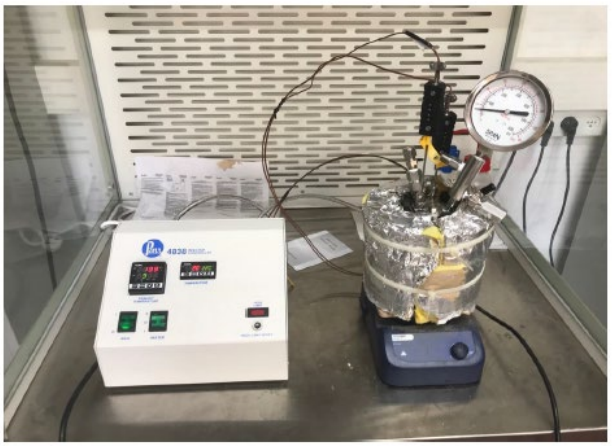

Figure 1. Experimental setup.

The refrigerant concentration absorbed in the liquid phase, ξ_R, is:

$$\xi_R = \frac{m_{RS}}{m_{RS} + m_{AS}} \tag{2}$$

The mass fraction of a refrigerant in a liquid solution is defined as the ratio of the refrigerant's mass in the solution to the total mass of the solution. The total mass of the solution is the sum of the refrigerant's mass and the absorbent's mass within the solution. However, these individual component masses within the solution are not measured directly. Mass balance equations are used to determine these values, which relate the measured total masses of refrigerant and absorbent to the respective masses of each component in both the liquid and gas phases of the system.

$$m_R = m_{RS} + m_{RG} \tag{3}$$

$$m_A = m_{AS} + m_{AG} \tag{4}$$

The liquid solution and the gaseous phase, V_G both occupy the total volume of the pressure vessel, V_T:

$$V_T = V_S + V_G \tag{5}$$

The volume of each phase consists of the volume of each of the components in that phase:

$$V_S = m_{RS} v_{RS} + m_{AS} v_{AS} \tag{6}$$

$$V_G = m_{RG} v_{RG} + m_{AG} v_{AG} \tag{7}$$

The specific volumes of the refrigerant were obtained from Engineering Equation Solver (EES) [26], and the absorbent in the liquid solution was obtained from [18]. The specific volumes of components in the gas phase are calculated using the Peng-Robinson equation of state. By combining Eq. (1), the masses of each component in each phase can be calculated, which enables the calculation of the concentration of the refrigerant in the liquid solution. Once the mass concentration of the refrigerant in the liquid solution was found, relationships between the equilibrium temperature and pressure can be determined by fitting to a polynomial function [18, 19], where p_{ij} are the polynomial coefficients are presented in Table 1.

$$p = \sum_{j=0}^{j} \sum_{i=0}^{i} p_{ij} \xi_R{}^i T^j \tag{8}$$

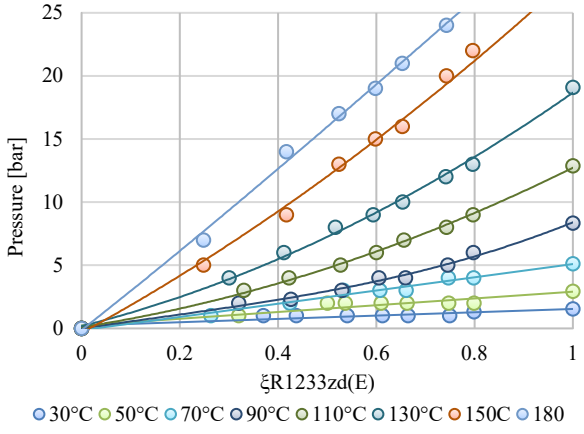

Figure 2. Pressure-temperature-concentration results in equilibrium.

Since the binary solution is not an ideal one, the enthalpy depends on the enthalpies and concentrations of each component and the excess enthalpy, h^E.

$$h = h_R \xi_R + h_A \left(1 - \xi_R\right) + h^E \tag{9}$$

Molar excess enthalpy, H^E, can be calculated based on the following expression:

$$H^E = \left(\frac{\partial \left(G^E / T \right)}{\partial \left(1/T \right)} \right)_{p,x} \tag{10}$$

Molar Gibbs free energy G^E is expressed as follows:

$$G^E = RT \left(x_A \ln \gamma_A + x_R \ln \gamma_R \right) \tag{11}$$

Molar concentrations x can be calculated based on each component's molar masses and mass concentrations:

$$x_R = \frac{\xi_R M_A}{\xi_R M_A + \xi_A M_R} \tag{12}$$

$$x_A = 1 - x_R \tag{13}$$

The activity coefficient for each component γ is:

$$\ln \gamma_R = A \left(1 + \frac{A}{B} \left(\frac{x_R}{x_A} \right) \right)^{-2} \tag{14}$$

$$\ln \gamma_A = B \left(1 + \frac{B}{A} \left(\frac{x_A}{x_R} \right) \right)^{-2} \tag{15}$$

Coefficients A and B are calculated based on Peng Robinson EOS.

The enthalpy of the liquid solution is expressed as a function of temperature T (in Celsius) and refrigerant mass concentration ξ_R [18,19], where h_{ij} are the coefficients of the polynomial function presented in Table 2 are calculated by linear regression:

$$h = \sum_{i=0}^{i} \sum_{j=0}^{j} h_{ij} \xi_R{}^j T^i \tag{16}$$

Figure 3 illustrates the enthalpy of the liquid solution at various temperatures as a function of refrigerant mass concentration.

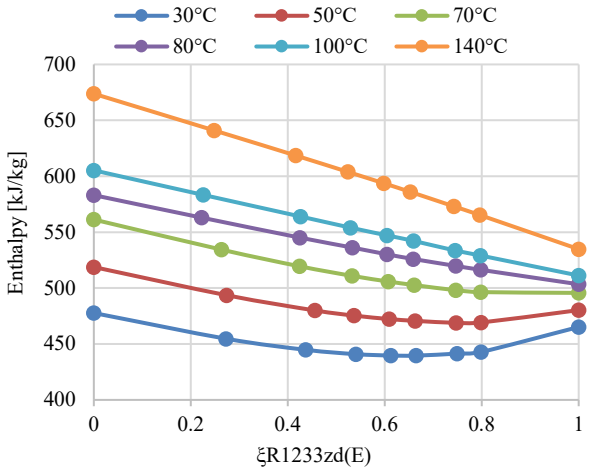

Figure 3. Enthalpy-temperature-concentration results in equilibrium.

All experimental measurements were subject to uncertainty, quantified based on instrument specifications and propagated into derived thermodynamic quantities. The masses of R1233zd(E) and DMAC were measured with an uncertainty of ±0.001g. Temperatures were measured using a Type-K thermocouple with an accuracy of ±0.5 °C, and pressures were recorded with a precision of ±1.0 kPa.

The refrigerant concentration in the liquid phase was not measured directly but was derived from equilibrium mass

and volume balances, utilizing specific volumes obtained from EES and EOS-based models. The uncertainty in concentration was propagated from mass and volume inputs and is estimated to be within a 2–4% relative error.

Polynomial regression models linking equilibrium pressure, temperature, and concentration exhibited high accuracy (R^2 = 0.995), with all fitted coefficients reported along with their standard errors and 95% confidence intervals. Similarly, enthalpy correlations as a function of temperature and concentration were developed using regression, and residual analysis confirmed the model's adequacy. Overall, all thermodynamic data presented include error bars or confidence intervals derived from both measurement and regression uncertainty. Since the values of error are relatively small, they are not presented on the graphs.

3. DAR Analysis Based on the Thermodynamic Properties

This research builds upon the DAR theoretical model of [15], combining with the obtained properties of the binary solution. The DAR system is presented in Figure 4.

This R1233zd(E)-DMAC-helium Diffusion Absorption Refrigeration (DAR) system simulation incorporates several key assumptions.

- Firstly, given that ambient air served as the cooling medium, the condenser and reservoir temperatures were assumed to be equal (T_6 = T_3). For the air-cooled condenser, $T_3 \approx 45°C$ and a corresponding total system pressure of 252 kPa.
- Within the generator, solution and vapor bubbles were assumed to exit at the same temperature.
- The heat input to the generator was assumed to heat the rich solution exclusively, neglecting any heat transfer to the returning weak solution.
- A 5°C temperature drop was assumed within the bubble pump for the rising solution and vapor bubbles (i.e., $T_{1c}=T_{1a}-5°C$).
- A $2°C$ temperature difference was assumed between stages 1a and 1b within the generator (i.e., $T_{1b}=T_{1a}-2°C$).
- It was assumed that Helium, containing residual R1233zd(E) entered the gas heat exchanger at $T_{5a}= 40°C$.
- The expansion temperature was assumed to be $T_{4c}=-35°C$.
- The temperature of the helium-R1233zd(E) mixture before expansion was assumed to be $5°C$ higher than after expansion (i.e., $T_{4a}=T_{4c}-5°C$).
- The gas mixture temperature at the evaporator outlet was assumed to be $T_{5b}=-5°C$.
- The bubble pump and the solution heat exchanger were assumed to be perfectly insulated.
- The contribution of hydrostatic pressure was considered negligible, and pressure drops within the piping system were neglected.
- The behavior of gas mixtures was assumed to follow the ideal gas law.
- The evaporator outlet was directly connected to the reservoir inlet. The R1233zd(E) leaving the rectifier at stage 2 was assumed to be pure, with negligible water vapor content.
- Adiabatic mixing was assumed to occur at the evaporator inlet. No absorption was assumed to take place within the reservoir.
- Assuming equilibrium conditions for both the rich solution entering the generator and the weak solution entering the absorber enabled the application of the pressure-temperature-concentration relationship.
- The enthalpies of a binary solution were calculated based on the enthalpy-temperature-concentration data.
- The mass and energy balances for each component were performed.
- The equations of the model are presented in [15].
- The system equations, combined with the properties of the new solution, were solved by EES.

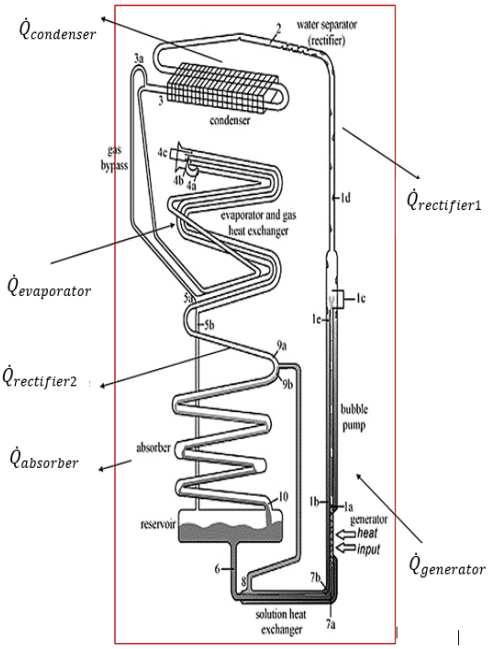

Figure 4. DAR system [15].

The COP of the DAR system is defined as:

$$COP = \frac{\dot{Q}_{evap}}{\dot{Q}_{gen}} \tag{17}$$

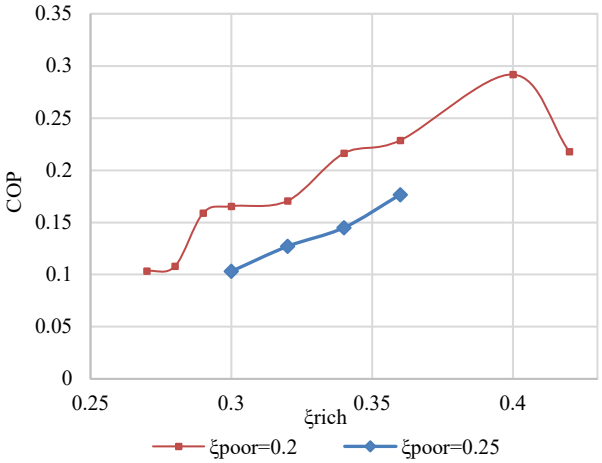

Figure 5. COP as a function of the refrigerant-rich solution concentration, for different poor solution concentrations.

Analyzing the system, we found that a rich solution concentration of 0.4 and the appropriate poor solution concentrations resulted in the highest COP values, reaching approximately 0.3. This is a typical COP range for a DAR system, as shown in Figure 5. We observed that lower poor solution concentrations (point 8) consistently led to higher

COPs. This trend aligns with our expectations, as lower concentrations improve absorption capacity due to reduced heat of mixing and enhanced mass transfer within the system, ultimately leading to more efficient refrigerant absorption and reduced energy consumption.

Our simulation results show that the maximum COP is achieved at a generator temperature of 114 °C, as illustrated in Figure 5. At temperatures below 114 °C, the model does not yield valid results due to insufficient thermal energy for effective desorption, meaning the system cannot operate properly. As the generator temperature increases beyond 114 °C, COP steadily decreases. This decline is attributed to the increased heat input required at higher temperatures, which outweighs the marginal gains in refrigerant circulation. Additionally, higher generator temperatures lead to greater thermodynamic irreversibilities and reduced system efficiency. Therefore, 114 °C represents both the minimum viable and optimal generator temperature under the given operating conditions with the R1233zd(E)–DMAC solution. This finding is consistent with previous work reported in [15], which also identified an optimal generator temperature range that balances desorption efficiency with system energy demands.

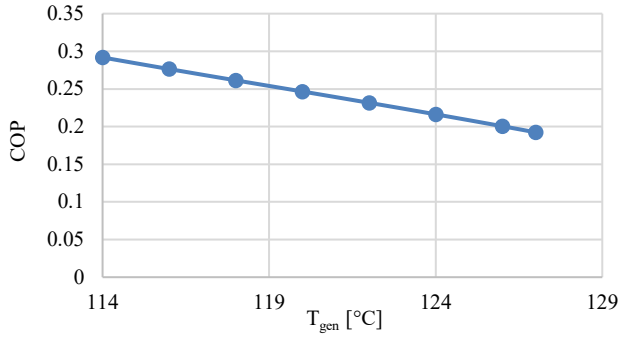

Figure 6. COP as a function of the generator temperature, for $\xi_{rich} = 0.4$ and $\xi_{poor} = 0.2$.

The circulation ratio *f* is defined as the ratio between the rich solution (point 6) and the mass flow rate of the pure R1233zd(E):

$$\boldsymbol{f} = \frac{\dot{m}_6}{\dot{m}_R} \tag{18}$$

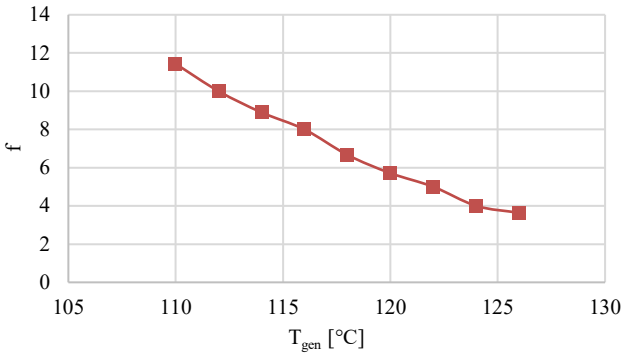

Figure 7. Circulation ratio as a function of the generator temperature.

Figure 7 shows how the circulation ratio changes with generator temperature in the DAR system. The circulation ratio represents the amount of working solution that must circulate in the system to produce a unit mass of refrigerant vapor. As generator temperature increases, the circulation ratio decreases, indicating improved refrigerant desorption efficiency. At higher temperatures, more refrigerant is separated from the solution, so less solution is needed to carry the same amount of refrigerant through the cycle. This trend suggests more efficient use of the working solution at elevated generator temperatures. However, it must be balanced against other effects—such as higher heat input and thermodynamic irreversibilities—which may reduce overall system efficiency. Therefore, optimizing generator temperature is essential for balancing good refrigerant recovery with energy efficiency.

In a DAR system, the refrigerant undergoes a cyclic process involving evaporation, absorption, desorption, and condensation. The T-s diagram is crucial for visualizing this cycle. Plotting the refrigerant's state points on this diagram can graphically represent the entire cycle and identify key points. The condensation (2–3), the sub-cooling (3–4a), the expansion (4a–4c), and the evaporation (4c–5b) processes for pure R1233zd(E) are described on a T–s diagram shown in Figure 8. The rich solution concentration was considered 0.4, and the poor solution concentration was 0.2; the generator temperature was 114°C. The figure clearly illustrates that evaporation occurs across partial pressures and temperatures.

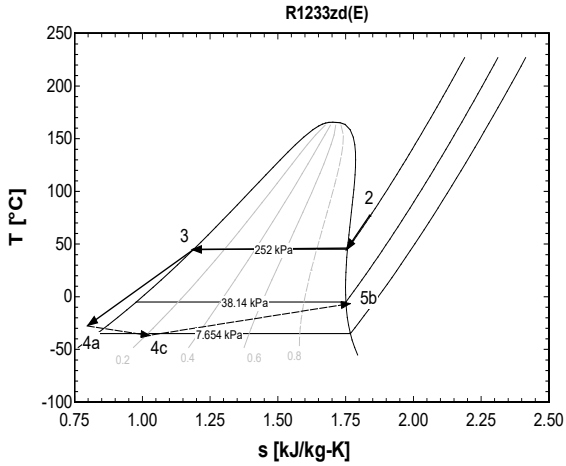

Figure 8. T-s diagram of R1233zd(E) in DAR system. $\xi_{rich} = 0.4$, $\xi_{poor} = 0.2$ and $T_{gen} = 114°C$.

4. Exergy Analysis

A second-law (exergy) analysis of the diffusion absorption refrigeration (DAR) system was conducted to complement the energy analysis and quantify the thermodynamic irreversibility within the system. This approach identifies the locations and magnitudes of exergy losses and evaluates overall efficiency based on useful energy quality [28]. In this study, the DAR system is modeled as a closed system with multiple heat sources, allowing second-law analysis to be performed without explicitly evaluating the entropy of the binary solution. The heat sources are presented in Figure 4.

The exergy balance of a closed steady-state system is expressed as:

$$\sum \dot{E}x_{in} - \sum \dot{E}x_{out} = \dot{E}x_{des} = \dot{I} \tag{19}$$

For systems exchanging only heat, the exergy associated with each thermal flow is calculated as:

Table 1. p_{ij} coefficients of R1233zd(E) and DMAC.

i, j	0	1	2	3	4	5
0	-35.68452	414.58381	-4215.90900	12843.67600	-14748.95800	4778.38790
1	3.08371	-33.71596	354.47720	-1122.05410	1388.77550	-587.27065
2	-0.10149	0.80804	-9.00146	29.16873	-36.52972	15.54918
3	0.00165	-0.00866	0.10412	-0.34617	0.43877	-0.18798

Table 2. h_{ij} coefficients of R1233zd(E) and DMAC.

i, j	0	1	2	3	4	5	6
0	-279000	42700	-356000	933000	-997000	372000	-279000
1	27800	-3390	28400	-75100	81000	-31000	27800
2	-1100	97.90000	-830	2200	-2380	911	-1100
3	22.10000	-1.34000	11.50000	-30.40000	33	-12.70000	22.10000
4	-0.24100	0.00874	-0.07580	0.20200	-0.21900	0.08440	-0.24100
5	0.00136	-0.00002	0.00019	-0.00052	0.00056	-0.00022	0.00136

$$\dot{E}x_Q = \left(1 - \frac{T_0}{T_B}\right)\dot{Q} \tag{20}$$

where, $\dot{Q}$ is the heat transferred, T_0 is the surrounding temperature, which is defined as 25°C or 298K, and T_B is the bulk temperature of the component. Positive $\dot{Q}$ represents heat input; negative $\dot{Q}$ represents heat rejection to the environment. For each component, exergy associated with heat flow is computed, and the sum of all flows allows determination of useful exergy, total input, and internal exergy destruction. These values are presented in Table 3 and in Figure 9.

Table 3. Exergy analysis results.

Component	Heat [W]	T_b [C]	T_0 [C]	Exergy [W]
Generator	323.5	114	25	74.37
Rectifier1	-33.9	90	25	-6.07
Condenser	-209.8	45	25	-13.19
Rectifier2	-37.6	40	25	-1.80
Absorber	-144.9	80	25	-22.57
Evaporator	102.8	-5	25	-11.50
Irreversibility				19.24

The exergy efficiency of the system is defined as the ratio between the exergy product and the total exergy input:

$$EXCOP = \frac{\dot{E}x_{evap}}{\dot{E}x_{gen}} \tag{21}$$

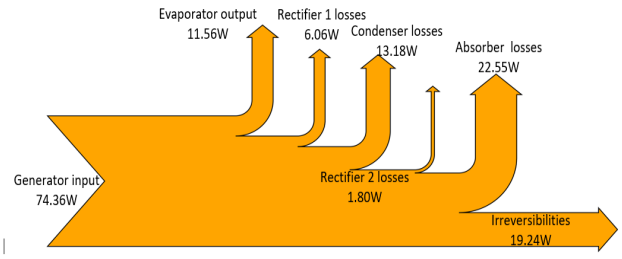

Figure 9. Exergy flow diagram.

The exergy efficiency of the R 1233 zd (E)–DMAC diffusion absorption refrigeration (DAR) system, calculated using a closed system framework, was approximately 15. 5%. This approach considers only the generator as the source of external exergy input, while the useful output is defined as the cooling effect provided by the evaporator. Exergy flows were computed using the external heat interactions at known bulk temperatures, eliminating the need for detailed entropy generation calculations for the binary working pair. All system components, including the solution heat exchangers and rectifiers, are considered to operate within the control volume, with their losses represented as internal exergy destruction. This formulation differs from open-system exergy evaluations commonly found in the literature, such as in the work of [28], who reported second-law efficiencies of 2.6%- 3.6% for a conventional ammonia–water–helium DAR system. The higher efficiency observed in our study can be attributed to the improved thermodynamic performance of the R1233zd(E)–DMAC working pair, lower operating pressures, and the exclusion of auxiliary system losses in the closed- system analysis. Our model treats heat exchangers as sources of internal irreversibility, allowing for a focused evaluation of component- level thermodynamic degradation. From an economic perspective, adopting R1233zd(E)–DMAC in DAR systems may offer notable advantages due to its compatibility with low- grade heat sources such as solar or industrial waste heat and its operation at lower pressures, potentially reducing material and manufacturing costs. Furthermore, the improved second-law performance enhances the effective utilization of available energy, a key consideration in energy- economic assessments for off- grid and sustainable cooling applications. These findings support the feasibility of developing novel working pairs and internal heat recovery designs to reduce irreversibilities and improve thermodynamic and economic performance.

5. Conclusions

This study comprehensively analyzes a DAR system utilizing R1233zd(E) as the refrigerant and DMAC as the absorbent. Experimental measurements were conducted to determine the thermodynamic properties of the R1233zd(E)-DMAC binary solution, including pressure-temperature-concentration and enthalpy-temperature-concentration data. These data were then integrated into a detailed DAR system model to evaluate performance.

Simulation results indicate that the system exhibits a reasonable COP, with optimal performance achieved at a generator temperature of 114°C, a rich solution concentration of 0.4, and a poor solution concentration of 0.2. Notably, this optimal generator temperature is significantly lower than that typically observed in conventional ammonia-water systems or other HFC-based DAR systems, such as those using R124. These results indicate that the system is well suited for operation with low-temperature heat sources such as solar thermal energy,

geothermal reservoirs, or industrial waste heat. A key advantage of the R1233zd(E)–DMAC working pair is its ability to operate at significantly lower generator temperatures and system pressures (252 kPa at a condenser temperature of 45°C) compared to traditional ammonia–water systems. This characteristic offers notable benefits regarding system design flexibility, material compatibility, and operational safety. While the COP values may be modest, the system's suitability for passive operation, environmental sustainability, and off-grid applications makes it a strong candidate for integration into decentralized or renewable-driven energy systems.

Increasing the generator temperature beyond the optimal point decreases COP due to increased heat input and reduced system efficiency. The analysis also shows that lower poor solution concentrations generally result in higher COPs, attributed to improved absorption capacity, reduced heat of mixing, and enhanced mass transfer. The circulation ratio decreased with increasing generator temperature, which can be attributed to increased vapor pressure and reduced solution density difference.

Additionally, a second-law (exergy) analysis was performed using a closed-system framework, where only the generator was considered as the external source of exergy input, and the evaporator's cooling effect was treated as the useful output. This analysis revealed an exergy efficiency of approximately 15.5%, notably higher than values reported in literature for traditional ammonia–water–inert gas systems, such as those by [28], who reported efficiencies between 2.6% and 3.6%. The improved performance in this study can be attributed to the superior thermodynamic behavior of the R1233zd(E)–DMAC pair, reduced operating pressures, and the focused treatment of internal irreversibilities, particularly within the heat exchangers and absorber. By modeling the DAR system as a closed control volume, the analysis avoids the need for detailed entropy characterization of the binary solution while capturing the significant sources of exergy destruction. From an economic standpoint, the ability to operate at lower pressures and utilize low-grade heat sources, such as solar thermal or industrial waste heat, positions this system as a cost-effective and environmentally favorable alternative. These findings emphasize the potential of exergy-based optimization and novel refrigerant pairs in enhancing the performance and sustainability of diffusion absorption cooling technologies. The system has strong potential for implementation in solar-driven cooling applications, especially in regions with limited access to electricity, where off-grid refrigeration is essential for preserving food and medicine. It is also well-suited for agricultural cold chains, enabling temperature control during post-harvest storage and transport in remote or rural areas. The use of the R1233zd(E)–DMAC working pair offers additional advantages due to its low global warming potential (GWP) and non-flammability, making it a safer and more environmentally responsible alternative to conventional refrigerants. These characteristics align with current sustainability goals and regulatory trends in refrigeration and cooling technologies.

This study focuses on testing the feasibility of using R1233zd(E) instead of ammonia, which is known to be toxic. However, caution is still advised in its application.

Future research should investigate this system's integration with renewable energy sources, particularly solar energy. This would be crucial to developing sustainable and environmentally friendly cooling solutions.

Acknowledgements
The authors have no acknowledgements to declare.

Conflict of Interest
Authors approve that to the best of their knowledge, there is not any conflict of interest or common interest with an institution/organization or a person that may affect the review process of the paper.

Credit Author Statement
Bella Gurevich: Conceptualization, Methodology, Software, Validation, Formal Analysis, Investigation, Resources, Data Curation, Writing - Original Draft, Visualization, Supervision, Project Administration, Funding Acquisition. **Amir Zohar:** Methodology and Software.

Nomenclature

A	First virial coefficient [-]
B	Second virial coefficient [-]
$\dot{E}$	Exergy $[W]$
f	Circulation ratio [-]
g	Gibbs free energy $[kJ/kg]$
h	Enthalpy $[kJ/kg]$
$\dot{I}$	Irreversibility $[W]$
M	Molar mass $[kJ/kmol]$
m	Mass $[kg]$
$\dot{m}$	Mass flow rate $[kg/s]$
p	Pressure $[bar]$
T	Temperature [℃], $[K]$
V	Volume $[m^3]$
v	Specific volume $[m^3/kg]$
x	Mole fraction in the liquid phase [-]
y	Mole fraction in gas phase [-]

Greek symbols

γ	Activity coefficient
ξ	Weight fraction in liquid phase
Φ	Correction factor
ψ	Weight fraction in gas phase

Subscripts

AG	Absorbent in gas phase
AS	Absorbent in liquid phase
evap	Evaporator
G	Gas
gen	Generator
i	Component index
R	Refrigerant
RG	Refrigerant in gas phase
RS	Refrigerant in liquid phase
S	Solution
T	Total

Superscript

E	Excess
L	Liquid
V	Vapor

References:

[1] B. C. von Platen and C. G. Munters, "Refrigerator," U.S. Patent 1 685 764, Sept. 25, 1928.

[2] Y. M. Park and R. E. Sonntag, "Thermodynamic properties of ammonia–water mixtures: A generalized equation-of-state approach," *ASHRAE Trans*., vol. 96, no. 1, pp. 150–159, 1990.

[3] O. M. Ibrahim, “Thermodynamic properties of ammonia–water mixtures,” in *ASHRAE Trans.: Symposia*, vol. 99, pt. 2, 1993, pp. 1495–1502.

[4] K. E. Herold, K. Hain, and M. J. Moran, “AMMWAT: A computer program for calculating the thermodynamic properties of ammonia and water mixtures using a Gibbs free energy formulation,” in *Proc. ASME Winter Annu. Meeting*, 1988, pp. 65–75.

[5] R. A. Heidemann and S. S. H. Rizvi, “Correlation of ammonia-water equilibrium data with various modified Peng-Robinson equations of state,” *Fluid Phase Equilibria*, vol. 29, pp. 439–446, Oct. 1986, doi: 10.1016/0378-3812(86)85042-7.

[6] P. C. Gillespie, W. V. Wilding, and G. M. Wilson, “Vapor-liquid equilibrium measurements on the ammonia-water system from 313 K to 589 K,” in *AIChE Symp. Ser.*, vol. 83, pp. 97–127, 1987.

[7] V. Abovsky, “Thermodynamics of ammonia water mixture,” *Fluid Phase Equilibria*, vol. 116, no. 1–2, pp. 170–176, Mar. 1996, doi: 10.1016/0378-3812(95)02884-6.

[8] B. Ziegler and C. Trepp, “Equation of state for ammonia-water mixtures,” *International Journal of Refrigeration*, vol. 7, no. 2, pp. 101–106, Mar. 1984, doi: 10.1016/0140-7007(84)90022-7.

[9] U. Jakob, U. Eicker, D. Schneider, A. H. Taki, and M. J. Cook, “Simulation and experimental investigation into diffusion absorption cooling machines for air-conditioning applications,” *Applied Thermal Engineering*, vol. 28, no. 10, pp. 1138–1150, Jul. 2008, doi: 10.1016/j.applthermaleng.2007.08.007.

[10] G. Starace and L. de Pascalis, “An enhanced model for the design of Diffusion Absorption Refrigerators,” *International Journal of Refrigeration*, vol. 36, no. 5, pp. 1495–1503, Aug. 2013, doi: 10.1016/j.ijrefrig.2013.02.016.

[11] P. Srikhirin and S. Aphornratana, “Investigation of a diffusion absorption refrigerator,” *Applied Thermal Engineering*, vol. 22, no. 11, pp. 1181–1193, Aug. 2002, doi: 10.1016/S1359-4311(02)00049-2.

[12] J. Chen, K. J. Kim, and K. E. Herold, “Performance enhancement of a diffusion-absorption refrigerator,” *International Journal of Refrigeration*, vol. 19, no. 3, pp. 208–218, Jan. 1996, doi: 10.1016/0140-7007(96)87215-X.

[13] N. Ben Ezzine, R. Garma, and A. Bellagi, “A numerical investigation of a diffusion-absorption refrigeration cycle based on R124-DMAC mixture for solar cooling,” *Energy*, vol. 35, no. 5, pp. 1874–1883, May 2010, doi: 10.1016/j.energy.2009.12.032.

[14] N. Ben Ezzine, R. Garma, and A. Bellagi, "A numerical investigation of a diffusion-absorption refrigeration cycle based on R124-DMAC mixture for solar cooling," *Energy*, vol. 35, no. 5, pp. 1874–1883, May 2010, doi: 10.1016/j.energy.2009.12.032.

[15] A. Zohar, M. Jelinek, A. Levy, and I. Borde, “Numerical investigation of a diffusion absorption refrigeration cycle,” *International Journal of Refrigeration*, vol. 28, no. 4, pp. 515–525, Jun. 2005, doi: 10.1016/j.ijrefrig.2004.11.003.

[16] A. Zohar, M. Jelinek, A. Levy, and I. Borde, “Performance of diffusion absorption refrigeration cycle with organic working fluids,” *International Journal of Refrigeration*, vol. 32, no. 6, pp. 1241–1246, Sep. 2009, doi: 10.1016/j.ijrefrig.2009.01.010.

[17] J. R. Sand, S. K. Fischer, and V. D. Baxter, *Energy and Global Warming Impacts of HFC Refrigerants and Emerging Technologies*. DOE/EIA-0035(97/03), Oak Ridge, TN, USA: Oak Ridge National Laboratory, 1997.

[18] I. Borde, M. Jelinek, and N. C. Daltrophe, “Absorption system based on the refrigerant R134a,” *International Journal of Refrigeration*, vol. 18, no. 6, pp. 387–394, Jul. 1995, doi: 10.1016/0140-7007(95)98161-D.

[19] I. Borde, M. Jelinek, and N. C. Daltrophe, “Working fluids for an absorption system based on R124 (2-chloro-1,1,1,2,-tetrafluoroethane) and organic absorbents,” *International Journal of Refrigeration*, vol. 20, no. 4, pp. 256–266, Jun. 1997, doi: 10.1016/S0140-7007(97)00090-X.

[20] V. Nair, “HFO refrigerants: A review of present status and future prospects.” *International Journal of Refrigeration*, vol. 122, pp. 156–170, Feb. 2021, doi: 10.1016/j.ijrefrig.2020.10.039.

[21] R. Akasaka, Y. Higashi, A. Miyara, and S. Koyama, “A fundamental equation of state for cis-1,3,3,3-tetrafluoropropene (R-1234ze(Z)),” *International Journal of Refrigeration*, vol. 44, pp. 168–176, Aug. 2014, doi: 10.1016/j.ijrefrig.2013.12.018.

[22] K. Tanaka and Y. Higashi, “Thermodynamic properties of HFO-1234yf (2,3,3,3-tetrafluoropropene),” *International Journal of Refrigeration*, vol. 33, no. 3, pp. 474–479, May 2010, doi: 10.1016/j.ijrefrig.2009.10.003.

[23] K. Tanaka, J. Ishikawa, and K. K. Kontomaris, “Thermodynamic properties of HFO-1336mzz (E) (trans-1,1,1,4,4,4-hexafluoro-2-butene) at saturation conditions,” *International Journal of Refrigeration*, vol. 82, pp. 283–287, Oct. 2017, doi: 10.1016/j.ijrefrig.2017.06.012.

[24] R. Akasaka and E. W. Lemmon, “An International Standard Formulation for *trans* -trans-1-Chloro-3,3,3-trifluoroprop-1-ene [R1233zd(E)] Covering Temperatures from the Triple-Point Temperature to 450 K and Pressures up to 100 MPa,” *Journal of Physical and Chemical Reference Data*, vol. 51, no. 2, Jun. 2022, doi: 10.1063/5.0083026.

[25] J. Yang, Z. Ye, B. Yu, H. Ouyang, and J. Chen, “Simultaneous experimental comparison of low-GWP refrigerants as drop-in replacements to R245fa for Organic Rankine cycle application: R1234ze(Z), R1233zd(E), and R1336mzz(E),” *Energy*, vol. 173, pp. 721–731, Apr. 2019, doi: 10.1016/j.energy.2019.02.054.

[26] S. A. Klein, Engineering Equation Solver (EES) V9. Madison, WI, USA: F-Chart Software, 2015.

[27] B. Gurevich, “Thermodynamic Properties of R1234yf and DMAC Binary Solution”, International Journal of Thermodynamics, vol. 27, no. 4, pp. 23–29, 2024, doi: 10.5541/ijot.1496861.

[28] B. Yıldız and M. Ersöz, “Exergoeconomic analysis of diffusion absorption refrigeration system using helium, hydrogen and ammonia,” *Energy*, vol. 63, pp. 400–407, 2013, doi: 10.1016/j.energy.2013.07.062.